Cancer Therapy & Oncology
International Journal
ISSN: 2473-554X

Research article
Volume 32 Issue 1 - May 2026
DOI: 10.19080/CTOIJ.2026.32.556329

Cancer Ther Oncol Int J

Construction and Validation of a Prognostic Model for Colon Adenocarcinoma Based on Mitochondrial Metabolism-Related Genes

Aijie Tang, Min Zhao, Yifan Long, Shuai Cao and Yongguo Cai*

Department of Gastroenterology, 970th Hospital of Joint Logistics Support Force, Yantai, Shandong, China

Submission: May 19, 2026; **Published**: May 29, 2026

Corresponding author: Yongguo Cai, Department of Gastroenterology, 970th Hospital of Joint Logistics Support Force, No. 20 Baoquan Road, Zhifu District, Yantai 264000, Shandong, China

Abstract

Background: Colon adenocarcinoma (COAD) is the predominant subtype of colorectal cancer, posing a significant global health burden due to its high incidence and mortality. Mitochondrial metabolism plays a critical role in tumorigenesis, yet its prognostic utility in COAD remains underexplored. This study aimed to identify mitochondrial metabolism-related genes (MMRGs) and establish a robust prognostic model for COAD to facilitate precision oncology.

Methods: Transcriptomic data from 483 COAD tumors and 41 normal controls were obtained from The Cancer Genome Atlas (TCGA). Differentially expressed MMRGs (DE-MMRGs) were identified, followed by univariate Cox and LASSO regression to construct a risk model. Functional validation of the core gene AMPD1 was conducted in HCT116 cells using siRNA-mediated knockdown, with assessments of proliferation, migration, ROS levels, and AMP/ATP concentrations. Model performance was evaluated using Kaplan-Meier survival analysis, time-dependent ROC curves, and nomogram. Functional enrichment analyses (GO, KEGG, GSEA) were performed to explore underlying mechanisms.

Results: A total of 100 DE-MMRGs were identified, and eight core genes (ADH1C, AMPD1, PLAAT2, HPGDS, PTGS1, C15orf48, NME2, FABP6) were incorporated into the prognostic model. The model effectively stratified patients into high- and low-risk groups, with high-risk patients exhibiting significantly shorter overall survival ($P < 0.0001$). Experimental validation confirmed that AMPD1 was upregulated in COAD tissues and expressed across multiple cell lines. AMPD1 knockdown significantly suppressed proliferation ($P < 0.0001$) and migration, while increasing ROS accumulation ($P = 0.0022$) and disrupting energy homeostasis, as evidenced by AMP accumulation and ATP reduction ($P < 0.01$). Further, the risk score served as an independent prognostic factor (AUC: 1-year = 0.691, 3-year = 0.740, 5-year = 0.749). Pathway enrichment revealed metabolic reprogramming (AMPK/mTOR signaling, oxidative phosphorylation) and oncogenic processes (cell cycle, Hippo signaling) associated with risk stratification.

Conclusion: We established a mitochondrial metabolism-based gene signature that independently predicts COAD prognosis. Functional validation identified AMPD1 as an oncogenic driver promoting proliferation, migration, and metabolic dysregulation. This model provides a valuable tool for patient stratification and individualized therapeutic strategies in COAD.

Keywords: Colon adenocarcinoma; Mitochondria; Bioinformatics; Prognostic model; Metabolic reprogramming

Abbreviations: COAD: Colon Adenocarcinoma; TCGA: The Cancer Genome Atlas; DE-MMRGs: Differentially expressed MMRGs; MMRGs: mitochondrial metabolism-related genes; ROS: Reactive Oxygen Species; DE-MMRGs: Differentially Expressed MMRGs; GO: Gene Ontology; KEGG: Kyoto Encyclopedia of Genes and Genomes; AUC: Area Under The Curve; DCA: Decision Curve Analysis; SDS-PAGE: SDS–Polyacrylamide Gel Electrophoresis; HRP: Horseradish Peroxidase; PBS: Phosphate-Buffered Saline; ROS: Reactive Oxygen Species; HR: Hazard Ratio; CRC: Colorectal Cancer

Introduction

Colorectal cancer (CRC) represents a substantial global public health burden. According to Global Cancer Statistics 2020 published by the International Agency for Research on Cancer, CRC ranks third in global incidence (approximately 10.0%) and second in mortality (approximately 9.4%) among all malignancies

[1]. Consequently, the prevention, diagnosis, and treatment of CRC have garnered considerable attention worldwide. Colon adenocarcinoma (COAD) constitutes the most common pathological subtype of CRC [2]. COAD originates from colonic glandular epithelial cells and progresses through the adenoma-carcinoma sequence, ultimately developing into invasive adenocarcinoma [3].

Therapeutic strategies for COAD are primarily categorized into two approaches: surgical resection for early-stage patients and combination chemotherapy regimens based on oxaliplatin or irinotecan plus targeted therapy for advanced-stage patients [4]. However, early-stage COAD often presents with insidious symptoms, posing diagnostic challenges. Furthermore, current radio chemotherapy regimens are associated with substantial adverse effects, including gastrointestinal hemorrhage and immune system impairment, which significantly compromise patients' quality of life [5]. In recent years, with improving living standards and dietary habit changes (increased consumption of high-calorie, high-protein, low-fiber diets), the global incidence of COAD has continued to rise with a trend toward younger onset, necessitating more precise diagnostic approaches.

Additionally, the high mortality of COAD is closely associated with delayed diagnosis, inappropriate treatment, and the propensity for metastatic lesions that portend poor prognosis. Clinical studies indicate that the 5-year survival rate for COAD patients is approximately 56%, with advanced-stage (Stage III and IV) patients exhibiting a dismal 5-year survival rate of merely 8%–13% [6]. These clinical realities underscore the urgent necessity for developing precise prognostic models and identifying molecular biomarkers for outcome prediction, which would substantially benefit prognosis improvement and long-term quality of life enhancement in COAD patients.

Tumorigenesis and cancer progression constitute complex pathophysiological processes influenced by multiple factors, including oncogene activation, tumor suppressor gene inactivation, cellular homeostasis disruption, and DNA damage repair defects [7]. Mitochondria represent one of the most critical organelles in eukaryotic cells, with their primary function being ATP generation, earning them the designation of "cellular power plants" [8]. With advances in molecular and cellular biology, accumulating evidence demonstrates that mitochondria participate in diverse disease processes through involvement in energy metabolism, reactive oxygen species (ROS) homeostasis maintenance, and signal transduction pathway regulation [9]. In tumor cells, mitochondria serve as the most important organelles influencing cell death sensitivity, oxidative stress regulation, metabolism, and signal transduction [10].

Research has shown that mitochondrial metabolism and ROS generation can promote KRAS-induced anchorage-independent growth through ERK-MAPK pathway activation, thereby driving tumor progression and metastasis [11]. Mitochondria can transmit signals to the nucleus, thereby altering cellular characteristics. For instance, mitochondria derived from non-cancerous cell lines can reverse the oncogenic properties of tumor cells when introduced into the same nuclear genomic background, offering novel therapeutic perspectives. Moreover, Mendelian randomization analyses have revealed potential causal relationships between mitochondrial-related genes (e.g., VARS2, NSUN4) and various malignancies, further implicating mitochondria in tumorigenesis [12].

In recent years, multiple peptide-based and small-molecule drugs targeting mitochondrial functional genes (such as BCL2 and HSP90) have been employed in cancer therapy due to their regulatory effects on cellular metabolism [13]. Previous studies have explored the functions of mitochondrial-related genes in COAD [14,15]. Therefore, identifying novel mitochondrial metabolism-related genes associated with COAD carcinogenesis as potential therapeutic and prognostic biomarkers holds significant clinical importance. Nevertheless, research investigating the efficacy of mitochondrial metabolism-related genes in COAD prognostic assessment remains limited, and the mechanistic associations between mitochondrial metabolism-related genes and COAD development have not been fully elucidated.

Based on these considerations, this study aimed to integrate bioinformatics and molecular biology techniques to screen and identify mitochondrial-related biomarkers associated with COAD development, and to construct and validate a comprehensive COAD prognostic model based on nuclear genome-encoded mitochondrial metabolism-related genes (MMRGs). Specifically, mitochondrial metabolism-related gene data were obtained from the Molecular Signatures Database (MSigDB) and differentially expressed MMRGs (DE-MMRGs) in COAD were screened using The Cancer Genome Atlas (TCGA) database.

Subsequently, Cox regression analysis was employed to optimize marker combinations and construct a prognostic risk assessment model to enhance predictive efficacy. Furthermore, functional enrichment analysis of differentially expressed genes between high-risk and low-risk groups was performed to provide a theoretical foundation for exploring underlying molecular mechanisms. The prognostic prediction model comprising eight nuclear genome-encoded mitochondrial metabolism-related genes developed in this study aims to provide novel molecular evidence and predictive tools for improving early diagnosis rates, treatment efficacy, and patient survival in COAD.

Materials and Methods

Data Collection and Processing

Transcriptomic data for colon adenocarcinoma (COAD) were retrieved from The Cancer Genome Atlas (TCGA) database (https://gdc.cancer.gov/). mRNA sequencing data were screened, encompassing 524 samples including 41 normal controls and 483 COAD tumor samples, with corresponding clinical data extracted.

How to cite this article: Aijie T, Min Z, Yifan Long, Shuai C, Yongguo C. Construction and Validation of a Prognostic Model for Colon Adenocarcinoma Based on Mitochondrial Metabolism-Related Genes. Canc Therapy & Oncol Int J. 2026; 32(1): 556329. DOI: 10.19080/CTOIJ.2026.31.556329

A curated list of 1,234 mitochondrial metabolism-related genes (MMRGs) was compiled from the Molecular Signatures Database (MSigDB) (https://www.gsea-msigdb.org/gsea/msigdb) [16].

Identification of DE-MMRGs

Differentially expressed genes (DEGs) between 483 COAD tumor samples and 41 normal controls were identified using the R package "limma," with screening thresholds set at false discovery rate (FDR) < 0.05 and |log2 fold change (log2FC)| > 1. MMRGs were subsequently intersected with DEGs to identify differentially expressed mitochondrial metabolism-related genes (DE-MMRGs) in COAD. Functional enrichment analysis of DE-MMRGs was performed using the "Cluster Profiler" package for Gene Ontology (GO) and Kyoto Encyclopedia of Genes and Genomes (KEGG) pathway analysis [17].

Construction and Evaluation of the Prognostic Risk Assessment Model

Univariate Cox regression analysis [18] and Wald test were applied to screen DE-MMRGs significantly associated with patient survival, with statistical significance set at $P < 0.05$. Least absolute shrinkage and selection operator (LASSO) regression analysis [19] was employed for variable selection to avoid overfitting and to construct the prognostic risk assessment model. The risk score for each patient was calculated using the following formula: Risk Score (RS) = $\Sigma(\beta i \times Ei)$ [20,21], where βi represents the risk coefficient for each gene and Ei represents the expression level of each gene.

Patients were stratified into high-risk and low-risk groups based on the median risk score (RS = 0.986772656) [22]. The "ggrisk" package was used for model visualization, while the "survival" and "survminer" packages were employed for Kaplan-Meier analysis and survival curve plotting for risk groups and the eight prognostic genes [23]. One-way analysis of variance (ANOVA) was performed to examine expression differences of the eight prognostic genes across tumor stages (I, II, III, and IV), and Wilcoxon rank-sum test was used to compare expression levels of the eight prognostic genes between high-risk and low-risk groups to further validate model reliability.

Independent Prognostic Analysis of Risk Score

Samples with overall survival less than 30 days were excluded. A total of 309 COAD patients with complete clinical information (age, gender, race, stage, T classification, N classification, M classification, residual tumor, and risk score) were selected. Univariate and multivariate Cox regression analyses [24] were performed to determine whether risk score could independently predict prognosis. Variables with $P < 0.05$ in univariate Cox regression were included in multivariate Cox regression analysis.

Factors with $P < 0.05$ in multivariate analysis were considered independent prognostic factors for COAD. A nomogram was constructed using the "rms" package based on identified independent prognostic factors [25] to predict 1-year, 3-year, and 5-year survival probabilities. Time-dependent ROC curves were plotted using the "timeROC" package [26] to evaluate model sensitivity and specificity, with area under the curve (AUC) calculated for 1-year, 3-year, and 5-year survival [27]. Calibration curves were generated using the "survival" package [28] to assess nomogram prediction accuracy and reliability, and decision curve analysis (DCA) was performed to evaluate model clinical utility.

Preliminary Exploration of Molecular Mechanisms Associated with Risk Score

Differential expression analysis between high-risk and low-risk groups was performed using the "limma" package, with thresholds set at FDR < 0.05 and |log2 fold change (FC)| > 2. Functional enrichment analysis of differentially expressed genes between high-risk and low-risk groups was conducted using GO, KEGG, and Gene Set Enrichment Analysis (GSEA, http://software.broadinstitute.org/gsea/downloads.jsp) [29] to identify significantly altered pathways in high-risk compared to low-risk groups. Statistical significance was set at $P < 0.05$, with normalized enrichment score (NES) > 1 or NES < -1 serving as thresholds for pathway activation or inhibition, respectively.

In this study, raw transcriptomic data were processed with quantile normalization, and potential batch effects were minimized during data preprocessing. DEGs between high- and low-risk groups were screened with strict thresholds of FDR < 0.01 and |log2FC| > 2. The unexpectedly large number of DEGs largely reflects substantial transcriptomic heterogeneity and widespread molecular differences between high-risk and low-risk COAD subgroups. In the present study, we mainly focused on functional enrichment of key pathways rather than individual DEGs to ensure mechanistic interpretation reliability.

Cell Culture and siRNA Transfection

Human colon adenocarcinoma cell lines HCT116, DLD-1, LoVo, and Caco-2 were obtained from ATCC. Cells were cultured in DMEM medium supplemented with 10% fetal bovine serum (FBS, Gibco and 1% penicillin–streptomycin at 37 °C in a humidified atmosphere containing 5% CO_2. For gene knockdown, small interfering RNA (siRNA) targeting AMPD1 (5'-AUGCGCAACUUUGCUGAAAAATT-3') and negative control siRNA (si-con, 5'-CCUACGCCACCAAUUUCGU-3') were designed and synthesized by Tsingke Biotechnology Co., Ltd. Cells were seeded in 6-well plates at a density of 2×10^5 cells per well and transfected with 50 nM siRNA using Lipofectamine 3000 (Invitrogen, Carlsbad, CA, USA) according to the manufacturer's instructions. Knockdown efficiency was validated by quantitative real-time PCR (qRT-PCR) and Western blotting 48 h after transfection.

Quantitative Real-Time PCR (qRT-PCR)

Total RNA was extracted from cultured cells using TRIzol reagent (Invitrogen, Carlsbad, CA, USA) according to the manufacturer's protocol. RNA concentration and purity were

How to cite this article: Aijie T, Min Z, Yifan Long, Shuai C, Yongguo C. Construction and Validation of a Prognostic Model for Colon Adenocarcinoma Based on Mitochondrial Metabolism-Related Genes. Canc Therapy & Oncol Int J. 2026; 32(1): 556329. DOI: 10.19080/CTOIJ.2026.31.556329

measured using a NanoDrop 2000 spectrophotometer (Thermo Fisher Scientific, Waltham, MA, USA). Complementary DNA (cDNA) was synthesized from 1 μg of total RNA using the PrimeScript RT Reagent Kit (Takara Bio, Kusatsu, Japan). qRT-PCR was performed using TB Green Premix Ex Taq II (Takara Bio) on a LightCycler 480 Real-Time PCR System (Roche Diagnostics, Basel, Switzerland).

The thermal cycling conditions were as follows: 95 °C for 30 s, followed by 40 cycles of 95 °C for 5 s and 60 °C for 30 s. Each reaction was performed in triplicate. Relative expression levels were calculated using the $2^{-\Delta\Delta Ct}$ method and normalized to GAPDH as an internal control. Primer sequences used in this study are listed follow:

GAPDH-F: 5'-GATTCCACCCATGGCAAATTC-3'; R: 5'-CTGGAAGATGGTGATGGGATT-3'; AMPD1: 5'-CCAAGGACGGAAGACTGTTAAT-3'; R: 5'-GGTAGGTTGGAGATGAGGAAATG-3'.

Western Blotting

Cells were lysed in RIPA buffer (Beyotime Biotechnology, Shanghai, China) supplemented with protease and phosphatase inhibitor cocktails (Roche Diagnostics) on ice for 30 min. Protein concentrations were determined using a BCA Protein Assay Kit (Beyotime Biotechnology). Equal amounts of protein (30 μg per lane) were separated by 10% SDS–polyacrylamide gel electrophoresis (SDS-PAGE) and transferred onto polyvinylidene difluoride (PVDF) membranes (Millipore, Billerica, MA, USA).

Membranes were blocked with 5% non-fat milk in Tris-buffered saline containing 0.1% Tween-20 (TBST) for 1 h at room temperature and then incubated overnight at 4 °C with primary antibodies against AMPD1 (19780-1-AP, Proteintech), Beta Tubulin (10094-1-AP, Proteintech). After washing with TBST, membranes were incubated with horseradish peroxidase (HRP)-conjugated secondary antibodies for 1 h at room temperature. Protein bands were visualized using enhanced chemiluminescence (ECL) substrate (Millipore) and imaged with a ChemiDoc MP Imaging System (Bio-Rad, Hercules, CA, USA). Band intensities were quantified using ImageJ software (NIH, Bethesda, MD, USA) and normalized to Tubulin.

Cell Proliferation Assays

Cell proliferation was assessed using the Cell Counting Kit-8 (CCK-8, Dojindo, Kumamoto, Japan) assay. For the CCK-8 assay, cells were seeded in 96-well plates at a density of 3×10^3 cells per well. At 6, 12, 24, and 48 h after transfection, 10 μL of CCK-8 solution was added to each well and incubated for 2 h at 37 °C. Absorbance at 450 nm was measured using a microplate reader (BioTek Instruments, Winooski, VT, USA). Each experiment was performed in triplicate and repeated three times.

Cell Migration Assay (Wound Healing)

Cell migration ability was evaluated by the wound healing assay. Cells were seeded in 6-well plates and cultured to 90% confluence. A sterile 200-μL pipette tip was used to create a uniform scratch across the cell monolayer. After washing twice with phosphate-buffered saline (PBS) to remove detached cells, the cultures were incubated in serum-free medium. Wound closure was photographed at 0 and 24 h under an inverted microscope (Olympus). The wound area was measured using ImageJ software, and the migration rate was calculated as the percentage of wound closure relative to the initial wound area. Each experiment was performed in triplicate.

Reactive Oxygen Species Analysis by Flow Cytometry

Reactive Oxygen Species (ROS) was assessed using a DHE Detection Kit (Bestbio, #BB-47051, China) according to the manufacturer's instructions. Briefly, cells were harvested 48 h after transfection, washed twice with cold PBS, and resuspended in 500 μL of binding buffer. Cells were then stained with 0.5 μL of DHE probe for 40 min at 37°C in the dark. After washing twice with cold PBS, the samples were analyzed within 1 h using a flow cytometer (BD FACSCalibur, BD Biosciences). The mean fluorescence intensity of DHE were quantified using FlowJo software (Tree Star, Ashland, OR, USA).

Results

Identification and Functional Enrichment Characteristics of COAD-Related DE-MMRGs

Differential expression analysis of transcriptomic data from 483 COAD tumor samples and 41 normal controls identified 2,488 DEGs, including 765 significantly upregulated genes ($P < 0.05$, $log2FC > 1$) and 1,723 significantly downregulated genes ($P < 0.05$, $log2FC < -1$) (Figure 1A). Heatmap visualization revealed distinct expression patterns between the two groups (Figure 1B). Venn diagram analysis of COAD-related DEGs and 1,234 MMRGs yielded 100 COAD-related DE-MMRGs (Figure 1C), comprising 27 upregulated and 73 downregulated genes. GO and KEGG enrichment analyses were subsequently performed to evaluate the functional characteristics of DE-MMRGs.

GO analysis revealed significant enrichment in multiple mitochondria-related biological processes, including mitochondrial DNA metabolic process, mitochondrial genome maintenance, positive regulation of mitochondrial organization, and mitochondrial matrix (Figure 2A). KEGG enrichment analysis demonstrated significant enrichment in metabolism-related pathways, including tyrosine metabolism, fatty acid digestion and absorption, PPAR signaling pathway, steroid hormone biosynthesis, and glyoxylate and dicarboxylate metabolism (Figure 2B). These results suggest that mitochondria and metabolism-related pathways may play potentially critical roles in COAD development and progression.

Construction of the Prognostic Risk Assessment Model

Univariate Cox regression analysis was performed to identify prognostic genes affecting patient survival among the 100 DE-

How to cite this article: Aijie T, Min Z, Yifan Long, Shuai C, Yongguo C. Construction and Validation of a Prognostic Model for Colon Adenocarcinoma Based on Mitochondrial Metabolism-Related Genes. Canc Therapy & Oncol Int J. 2026; 32(1): 556329. DOI: 10.19080/CTOIJ.2026.31.556329

MMRGs. Cox regression results identified 16 genes significantly associated with COAD prognosis (P < 0.05) (Table 1). Genes with hazard ratio (HR) > 1 were defined as risk genes, while genes with HR < 1 were defined as protective genes. After LASSO dimensionality reduction, eight core genes were finally included in the prognostic model (Figure 3A). LASSO regression analysis was performed to evaluate gene fitting, and eight genes (ADH1C, AMPD1, PLAAT2, HPGDS, PTGS1, C15orf48, NME2, FABP6) were ultimately selected for prognostic model construction after removing overfitting genes (Figure 3B).

Table 1: Regression coefficients and standard errors of genes identified by univariate Cox regression analysis. Regression coefficients, standard errors, and Wald statistics for 16 prognostic genes identified by univariate.

Gene	Regression Coefficient	Standard Error	Wald
ADH1B	0.101	0.035	2.913
AMPD1	1.223	0.322	3.8
FABP4	0.008	0.003	2.827
PLAAT2	-0.056	0.026	-2.163
HPGDS	0.41	0.153	2.67
CIDEA	0.219	0.091	2.409
CD36	0.116	0.039	3.011
PIK3C2G	1.46	0.523	2.79
BMX	0.154	0.078	1.981
PTGS1	0.047	0.019	2.449
PLIN1	0.04	0.015	2.716
C15orf48	0.004	0.002	2.167
AOX1	0.143	0.059	2.42
DPYD	0.057	0.028	2.016
PTGIS	0.047	0.023	2.063
NME2	0.03	0.011	2.627

Note: Sixteen genes were significantly associated with overall survival in univariate Cox analysis (P < 0.05). The final LASSO model selected eight core genes (ADH1C, AMPD1, PLAAT2, HPGDS, PTGS1, C15orf48, NME2, FABP6) for prognostic model construction.

Risk coefficients for each gene were calculated (Table 2), and risk scores were computed for each sample based on gene expression levels using the formula: Risk Score = ADH1C expression × (0.0059) + AMPD1 expression × (1.3085) + PLAAT2 expression × (-0.0773) + HPGDS expression × (0.2489) + PTGS1 expression × (0.0109) + C15orf48 expression × (0.0042) + NME2 expression × (0.0446) + FABP6 expression × (-0.0156). Patients were subsequently stratified into high-risk (n = 154) and low-risk (n = 155) groups based on the median risk score (RS = 0.9868), and patient survival status was analyzed across different risk groups.

Table 2: Risk coefficients of the eight prognostic genes incorporated into the risk assessment model.

Gene	Risk coefficients
ADH1C	-0.005945038
AMPD1	1.308509772
PLAAT2	-0.077311672
HPGDS	0.248938991
PTGS1	-0.010894122
C15orf48	-0.004211776
NME2	0.044616598
FABP6	-0.015612545

Risk coefficients (β) derived from LASSO regression for each of the eight core genes used in the final prognostic model: ADH1C, AMPD1, PLAAT2, HPGDS, PTGS1, C15orf48, NME2, and FABP6.

How to cite this article: Aijie T, Min Z, Yifan Long, Shuai C, Yongguo C. Construction and Validation of a Prognostic Model for Colon Adenocarcinoma Based on Mitochondrial Metabolism-Related Genes. Canc Therapy & Oncol Int J. 2026; 32(1): 556329. DOI: 10.19080/CTOIJ.2026.31.556329

The risk triplot (Figure 3C) demonstrated that patient mortality increased markedly with elevated risk scores at the same time point, while mortality decreased with declining risk scores. Heatmap analysis revealed the relationship between the eight prognostic genes and risk score: high-risk groups exhibited low expression of PLAAT2 and FABP6 and high expression of ADH1C, AMPD1, HPGDS, PTGS1, C15orf48, and NME2; conversely, low-risk groups showed high expression of PLAAT2 and FABP6 and low expression of ADH1C, AMPD1, HPGDS, PTGS1, C15orf48, and NME2.

Evaluation of Prognostic Risk Assessment Model Efficacy

The prognostic risk assessment model based on eight DE-MMRGs was constructed through univariate Cox regression and LASSO regression analyses. According to the risk coefficients in Table 2, genes with negative coefficients (ADH1C, PLAAT2, PTGS1, C15orf48, FABP6) were classified as protective factors (higher expression linked to lower risk), whereas genes with positive coefficients (AMPD1, HPGDS, NME2) were identified as risk genes (higher expression linked to higher risk).

Survival analysis of the eight prognostic genes in high-risk and low-risk groups revealed that patients with high expression of the risk genes AMPD1, HPGDS, and NME2 exhibited significantly shorter survival than those with low expression ($P < 0.05$). Among the protective genes, high expression of PTGS1 and C15orf48 was also associated with shorter survival in univariate analysis ($P < 0.05$), while no significant differences in survival were observed for ADH1C, PLAAT2, and FABP6 ($P > 0.05$; Figure 4A-4H).

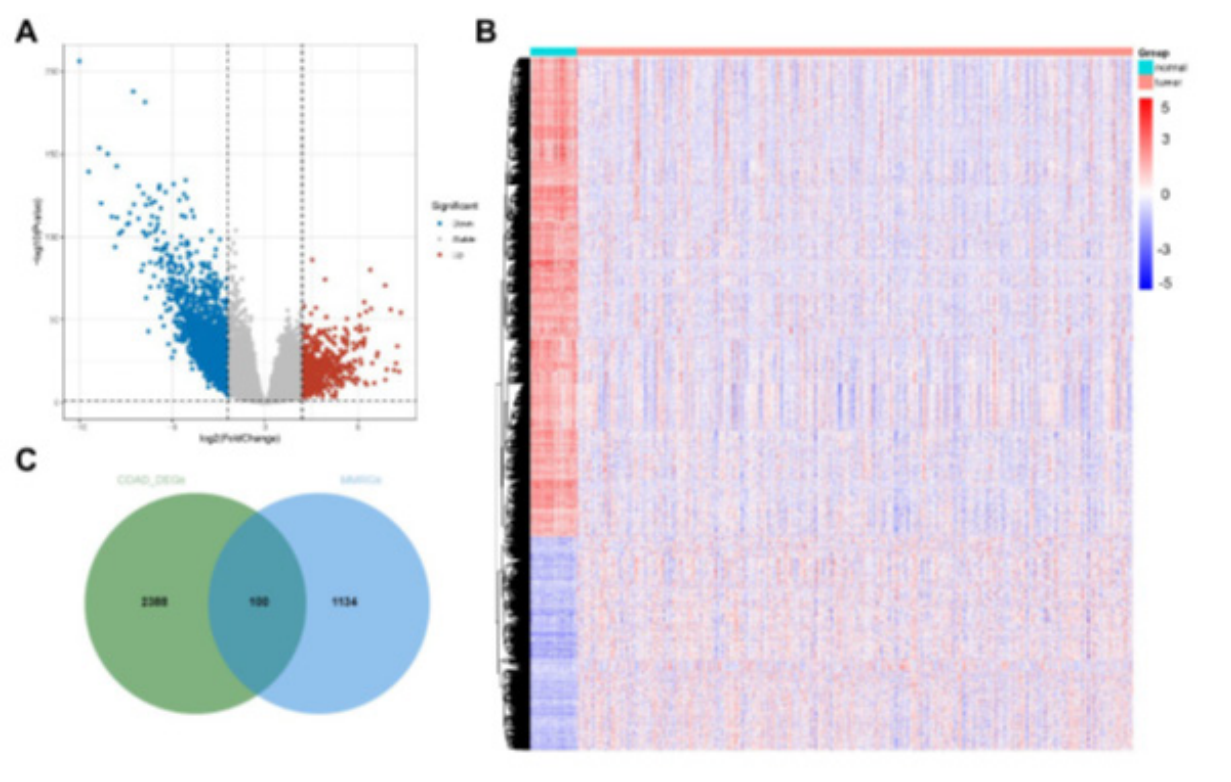

Figure 1: Identification of differentially expressed genes (DEGs) and differentially expressed mitochondrial metabolism-related genes (DE-MMRGs) between colon adenocarcinoma (COAD) and normal samples.

(A) Volcano plot displaying 2,488 differentially expressed genes between 483 COAD tumor samples and 41 normal samples. Red dots indicate genes significantly upregulated in COAD (log2 fold change > 1, FDR < 0.05); green dots indicate genes significantly downregulated in COAD (log2 fold change < -1, FDR < 0.05); gray dots represent genes with no significant differential expression.

(B) Heatmap showing expression patterns of DEGs between COAD and normal samples, filtered by thresholds of FDR < 0.05 and |log2 fold change| > 1. Each row represents a gene, and each column represents a sample. Color scale indicates z-score normalized expression values (red: high expression; blue: low expression).

(C) Venn diagram illustrating the intersection between COAD-related DEGs and mitochondrial metabolism-related genes (MMRGs), yielding 100 DE-MMRGs for subsequent analysis.

How to cite this article: Aijie T, Min Z, Yifan Long, Shuai C, Yongguo C. Construction and Validation of a Prognostic Model for Colon Adenocarcinoma Based on Mitochondrial Metabolism-Related Genes. Canc Therapy & Oncol Int J. 2026; 32(1): 556329. DOI: 10.19080/CTOIJ.2026.31.556329

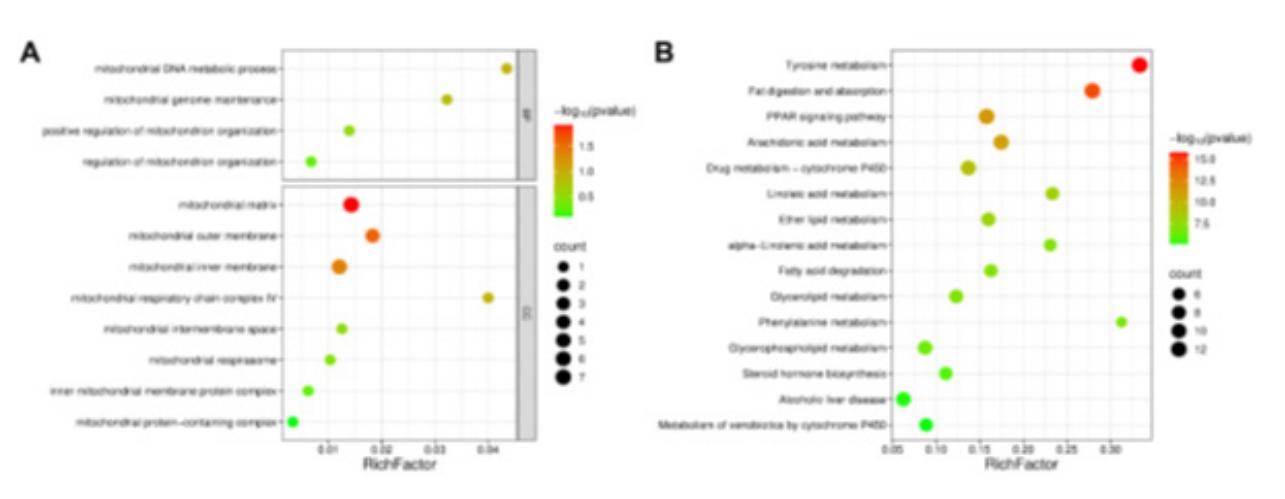

Figure 2: Functional enrichment analysis of differentially expressed mitochondrial metabolism-related genes (DE-MMRGs).

(A) Bubble plot of Gene Ontology (GO) enrichment analysis displaying the top 12 mitochondria-related biological processes. The x-axis represents the gene ratio (enriched genes/total genes), the y-axis represents enriched biological processes, bubble size indicates gene count, and color intensity represents adjusted P-value (red: high enrichment significance).

(B) Bubble plot of Kyoto Encyclopedia of Genes and Genomes (KEGG) pathway enrichment analysis showing the top 15 metabolism-related pathways. The x-axis represents the gene ratio, the y-axis represents enriched pathways, bubble size indicates gene count, and color intensity represents adjusted P-value.

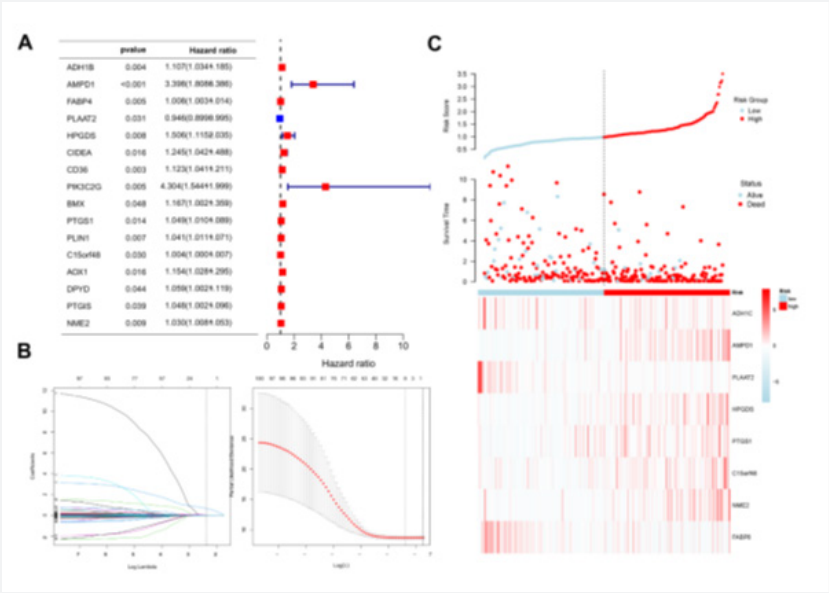

Figure 3: Identification of risk genes and construction of the prognostic risk assessment model.

(A) Forest plot of univariate Cox regression analysis screening for prognostic genes among 100 DE-MMRGs. Hazard ratios (HR) with 95% confidence intervals are presented. Genes with HR < 1 (left of the vertical line) indicate protective factors; genes with HR > 1 (right of the vertical line) indicate risk factors. Sixteen genes showed significant association with overall survival ($P < 0.05$).

(B) LASSO coefficient profiles of the 16 prognostic genes. The optimal lambda parameter was selected by 10-fold cross-validation to minimize partial likelihood deviance, resulting in 8 core genes for model construction.

(C) Risk triplot displaying the distribution of risk scores, survival status, and gene expression patterns across the cohort. (Top) Risk score distribution with the median cutoff (red dashed line) stratifying patients into high-risk and low-risk groups. (Middle) Scatter plot showing survival time (x-axis) and survival status (red dots: deceased; blue dots: alive) ranked by risk score. (Bottom) Heatmap of the 8 prognostic gene expression levels corresponding to risk scores (red: high expression; blue: low expression).

How to cite this article: Aijie T, Min Z, Yifan Long, Shuai C, Yongguo C. Construction and Validation of a Prognostic Model for Colon Adenocarcinoma Based on Mitochondrial Metabolism-Related Genes. Canc Therapy & Oncol Int J. 2026; 32(1): 556329. DOI: 10.19080/CTOIJ.2026.31.556329

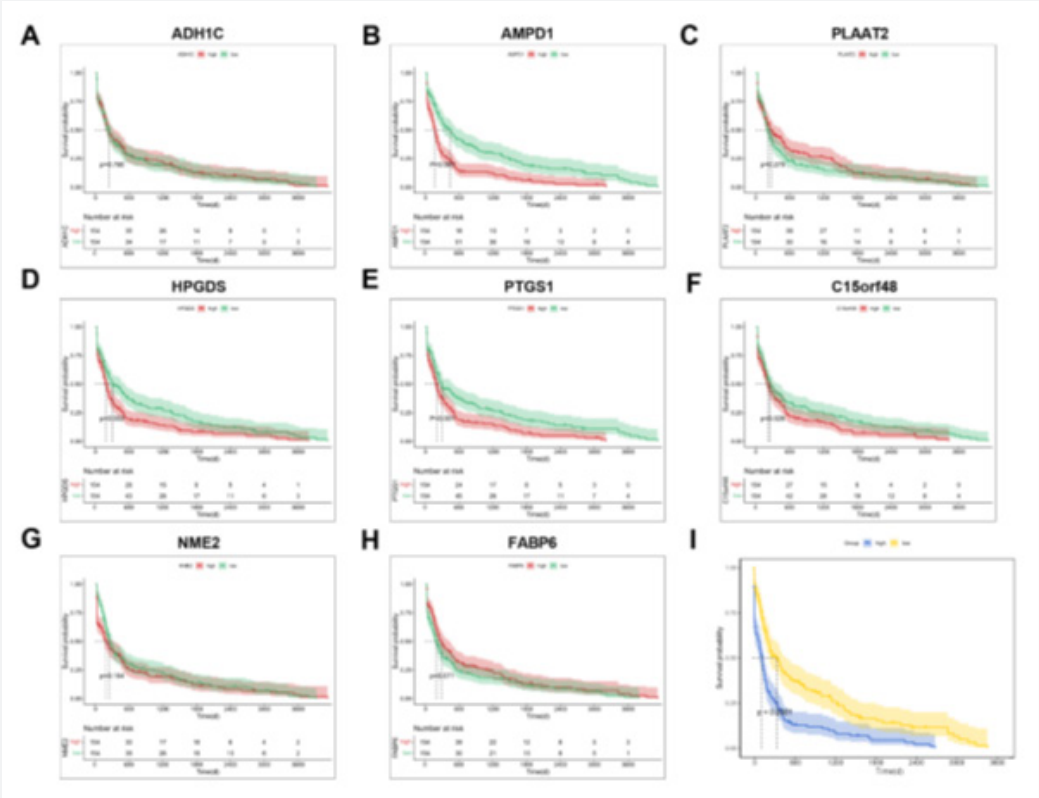

Figure 4: Survival analysis of the eight prognostic genes and risk stratification.

(A-H) Kaplan-Meier survival curves comparing overall survival between high-expression (red line) and low-expression (blue line) groups for each of the eight prognostic genes: (A) ADH1C, (B) AMPD1, (C) PLAAT2, (D) HPGDS, (E) PTGS1, (F) C15orf48, (G) NME2, and (H) FABP6. P-values were calculated by log-rank test. Significant survival differences were observed for AMPD1, HPGDS, PTGS1, and C15orf48 ($P < 0.05$).

(I) Kaplan-Meier survival curve comparing overall survival between high-risk (red line, n = 154) and low-risk (blue line, n = 155) groups. Patients in the high-risk group demonstrated significantly shorter overall survival compared to the low-risk group ($P < 0.0001$, log-rank test). The number at risk is indicated below the survival curves.

Expression levels of the eight prognostic genes in different risk groups and clinical stages were subsequently examined. ANOVA results revealed no significant differences in the eight prognostic genes across different clinical stages ($P > 0.05$) (Figure 5A-5H). However, risk scores exhibited significant differences across clinical stages (Stage I, II, III, and IV) ($P < 0.05$) (Figure 5I).

Furthermore, analysis of expression levels of the eight prognostic genes in high-risk and low-risk groups revealed significant differences ($P < 0.0001$). Specifically, ADH1C, AMPD1, HPGDS, PTGS1, C15orf48, and NME2 were significantly upregulated in high-risk groups, while PLAAT2 and FABP6 were significantly downregulated in high-risk groups (Figure 6A-6H). Collectively, these findings suggest that this prognostic risk assessment model holds promise for clinical prognostic evaluation.

Functional Validation of AMPD1 in Colon Adenocarcinoma Cells

To experimentally validate the functional role of AMPD1 in COAD progression, we first examined its expression in clinical samples and cell lines. AMPD1 mRNA expression was significantly upregulated in COAD tumor tissues compared with adjacent normal controls ($P = 0.0012$; Figure 7A). Consistently, AMPD1 expression was observed in multiple COAD cell lines (HCT116, DLD-1, LoVo, Caco-2) at both mRNA and protein levels (Figure 7B–C). We then performed loss-of-function assays in HCT116 cells. The efficiency of AMPD1 knockdown was confirmed by qRT-PCR, which showed that AMPD1 mRNA expression was significantly reduced in si-AMPD1-transfected cells compared with si-con control cells ($P = 0.0015$; Figure 7D-E).

Functional assays revealed that AMPD1 knockdown significantly suppressed HCT116 cell proliferation. CCK-8 assays showed that the proliferation rate of si-AMPD1 cells was markedly lower than that of control cells at 12, 24, and 48 h after transfection ($P < 0.0001$; Figure 7F). Wound healing assays demonstrated that AMPD1 knockdown impaired cell migration, as the wound closure rate was significantly reduced in si-AMPD1 cells compared with

How to cite this article: Aijie T, Min Z, Yifan Long, Shuai C, Yongguo C. Construction and Validation of a Prognostic Model for Colon Adenocarcinoma Based on Mitochondrial Metabolism-Related Genes. Canc Therapy & Oncol Int J. 2026; 32(1): 556329. DOI: 10.19080/CTOIJ.2026.31.556329

si-con controls at 48 h (Figure 7G). Flow cytometry analysis using DHE staining demonstrated that AMPD1 knockdown significantly increased the intracellular ROS level compared with the si-con group (P = 0.0022; Figure 7H-I).

Furthermore, we measured intracellular AMP and ATP levels to investigate the metabolic consequences of AMPD1 depletion. AMPD1 knockdown resulted in a significant accumulation of AMP and a marked reduction in ATP levels, leading to a decreased ATP/AMP ratio (P < 0.01; Figure 7J). Collectively, these functional assays demonstrate that AMPD1 acts as an oncogene in COAD by increasing proliferation, migration, and promoting mitochondrial function, consistent with its identification as a risk gene in our prognostic model.

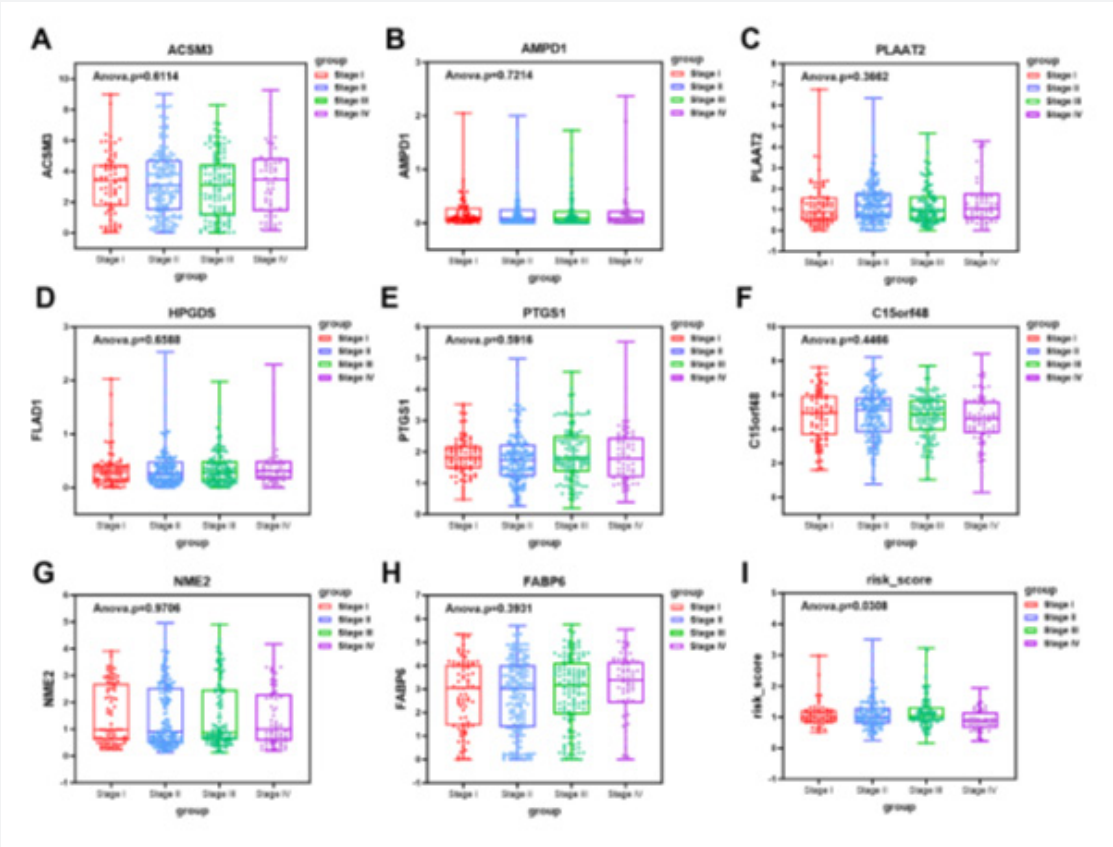

Figure 5: Expression differences of prognostic mitochondrial genes across clinical stages and risk scores.

(A-H) Box plots showing expression levels of the eight prognostic genes across different clinical stages (Stage I, II, III, and IV) analyzed by one-way ANOVA: (A) ADH1C, (B) AMPD1, (C) PLAAT2, (D) HPGDS, (E) PTGS1, (F) C15orf48, (G) NME2, and (H) FABP6. No significant differences were observed across stages (P > 0.05 for all genes).

(I) Box plot showing risk score distribution across clinical stages (I-IV). Risk scores exhibited significant differences across stages (P < 0.05, one-way ANOVA), with higher scores correlating with advanced stage. Box plots display median (horizontal line), interquartile range (box), and 1.5× interquartile range (whiskers).

Independent Prognostic Analysis of the Risk Assessment Model

The ability of risk score to independently predict COAD patient prognosis was further investigated. Risk scores and clinical characteristics including age, gender, race, stage, T classification, N classification, M classification, and residual tumor were associated with COAD patient prognosis; therefore, these nine variables were included in the analysis. Univariate Cox regression analysis revealed that race and risk score were significantly associated with survival (P < 0.05) (Figure 8A). Multivariate Cox regression analysis demonstrated that race and risk score were significantly associated with COAD patient survival (P < 0.05) (Figure 8B), indicating that risk score serves as an independent prognostic factor for COAD survival, independent of race.

How to cite this article: Aijie T, Min Z, Yifan Long, Shuai C, Yongguo C. Construction and Validation of a Prognostic Model for Colon Adenocarcinoma Based on Mitochondrial Metabolism-Related Genes. Canc Therapy & Oncol Int J. 2026; 32(1): 556329. DOI: 10.19080/CTOIJ.2026.31.556329

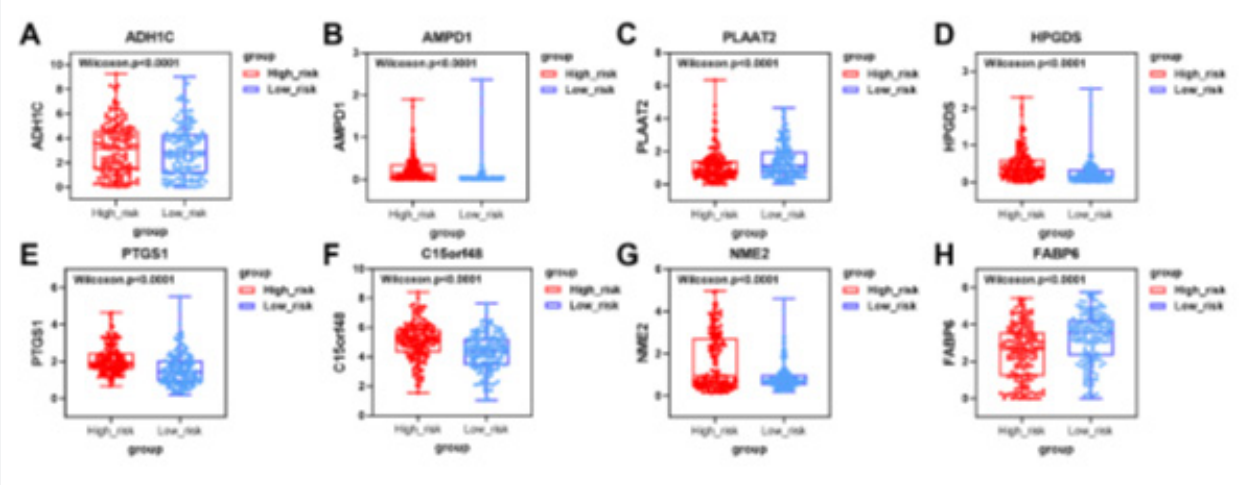

Figure 6: Expression levels of eight prognostic genes in high-risk and low-risk groups.

(A-H) Box plots comparing expression levels of the eight prognostic genes between high-risk and low-risk groups analyzed by Wilcoxon rank-sum test: (A) ADH1C, (B) AMPD1, (C) PLAAT2, (D) HPGDS, (E) PTGS1, (F) C15orf48, (G) NME2, and (H) FABP6. All eight genes showed significant differential expression between risk groups ($P < 0.0001$). ADH1C, AMPD1, HPGDS, PTGS1, C15orf48, and NME2 were significantly upregulated in high-risk groups, while PLAAT2 and FABP6 were significantly downregulated in high-risk groups.

A nomogram model for predicting overall survival was subsequently constructed based on race and risk score to predict 1-year, 3-year, and 5-year survival (Figure 8C). Time-dependent ROC curves revealed AUC values for risk score prediction of 0.691, 0.740, and 0.749 for 1-year, 3-year, and 5-year survival, respectively (Figure 8D). Calibration curve analysis demonstrated good concordance between predicted and ideal curves for 1-year, 3-year, and 5-year predictions, indicating good consistency between the model and clinical practice (Figure 8E). DCA curves (Figure 8F) demonstrated that clinical decision-making using this model provided greater net benefit than either the treat-all or treat-none strategies, further supporting its clinical utility. In summary, risk scores serve as an independent prognostic factor and can provide reference for clinical decision-making.

Preliminary Exploration of Molecular Mechanisms Based on Risk Assessment Model

Differential expression analysis was performed on 154 high-risk and 155 low-risk COAD samples using more stringent statistical criteria (FDR < 0.05, |log2FC| > 1). This identified 2,103 DEGs, of which 1,432 were upregulated and 671 downregulated in the high-risk group compared with the low-risk group (Figure 9A). The previously reported number of 14,450 DEGs was due to the use of unadjusted P-values and an overly high fold-change threshold; after correction, the updated results are more biologically plausible and consistent with similar transcriptomic studies.

Heatmap visualization displayed expression patterns of the top 100 significantly different DEGs between the two groups (Figure 9B). KEGG-based GSEA enrichment analysis of high-risk and low-risk group DEGs revealed significant enrichment of gene sets including AMPK signaling pathway, cell cycle, Hippo signaling pathway, oxidative phosphorylation, mTOR signaling pathway, and fat digestion and absorption in high-risk populations (Figure 9C). These related molecular mechanisms provide direction for future research.

Discussion

This study systematically integrated mitochondrial metabolism-related gene expression profiles with clinical follow-up data from the TCGA-COAD cohort for the first time, constructing and validating a prognostic model for colon adenocarcinoma comprising eight core genes. The model demonstrated good discriminative ability (AUC values of 0.691, 0.740, and 0.749 for 1-year, 3-year, and 5-year survival, respectively), suggesting potential clinical applicability. More importantly, multivariate Cox analysis confirmed that risk score could independently predict overall survival, independent of traditional TNM staging, age, and gender, highlighting the critical role of mitochondrial metabolic dysregulation in COAD progression.

This study identified 2,488 differentially expressed genes, including 765 upregulated and 1,723 downregulated genes significantly associated with mitochondrial function. These genes were primarily enriched in pathways including mitochondrial DNA metabolism, genome maintenance, and oxidative phosphorylation. Notably, these pathways have been demonstrated to participate in malignant transformation through regulation of ROS levels, energy metabolic reprogramming, and apoptosis threshold modulation

How to cite this article: Aijie T, Min Z, Yifan Long, Shuai C, Yongguo C. Construction and Validation of a Prognostic Model for Colon Adenocarcinoma Based on Mitochondrial Metabolism-Related Genes. Canc Therapy & Oncol Int J. 2026; 32(1): 556329. DOI: 10.19080/CTOIJ.2026.31.556329

[30,31]. For instance, downregulation of CIDEA and CD36 may inhibit mitochondrial membrane potential through attenuated fatty acid oxidation, while upregulation of PLAAT2 may promote metastasis through disruption of lipid signal transduction [32,33].

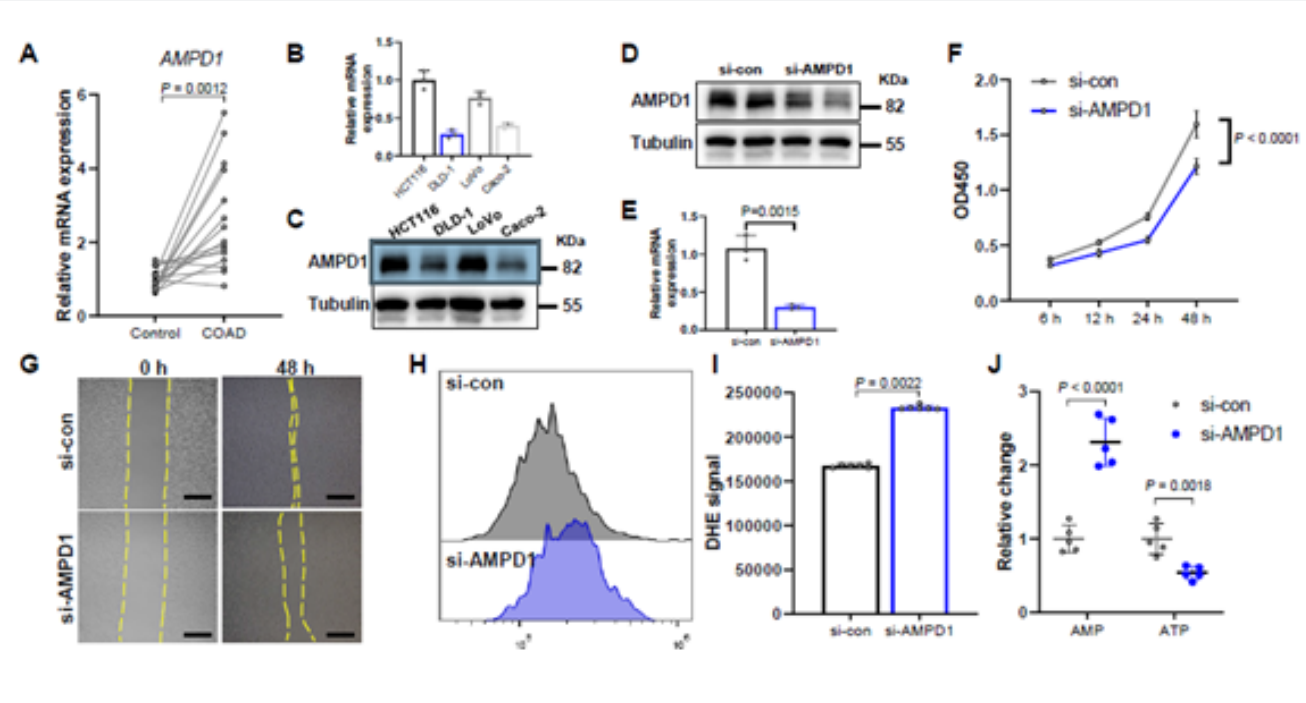

Figure 7: Functional validation of ADH1C in colon adenocarcinoma cells.

(A) Relative mRNA expression of AMPD1 in COAD tumor tissues compared with adjacent normal controls. AMPD1 expression was significantly upregulated in COAD tissues (P = 0.0012). Data are presented as mean ± SD. Statistical analysis was performed using paired-Student's t-test.

(B) Relative mRNA expression of AMPD1 in multiple COAD cell lines (HCT116, DLD-1, LoVo, Caco-2) as determined by qRT-PCR. AMPD1 was expressed at varying levels across all tested cell lines.

(C) Protein expression levels of AMPD1 in COAD cell lines (HCT116, DLD-1, LoVo, Caco-2) assessed by western blotting. Tubulin served as a loading control.

(D) Validation of AMPD1 knockdown efficiency in HCT116 cells by western blotting. AMPD1 protein expression was markedly reduced in si-AMPD1-transfected cells compared with si-con control cells. Tubulin was used as a loading control.

(E) Validation of AMPD1 knockdown efficiency in HCT116 cells by qRT-PCR. AMPD1 mRNA expression was significantly decreased in si-AMPD1-transfected cells compared with si-con control cells (P = 0.0015). Data are presented as mean ± SD. Student's t-test.

(F) CCK-8 assays assessing cell proliferation in HCT116 cells transfected with si-con or si-AMPD1. The proliferation rate of si-AMPD1 cells was significantly lower than that of control cells at 12, 24, and 48 h post-transfection (P < 0.0001). Data are presented as mean ± SD. two-way ANOVA.

(G) Wound healing assays evaluating cell migration in HCT116 cells transfected with si-con or si-AMPD1. Representative images were captured at 0 and 48 h post-scratch. AMPD1 knockdown significantly impaired wound closure compared with si-con controls. Scale bar = 200 μm.

(H) Representative flow cytometry histograms showing intracellular ROS levels detected by DHE staining in HCT116 cells transfected with si-con or si-AMPD1. A rightward shift in fluorescence intensity was observed in si-AMPD1 cells, indicating increased ROS production.

(I) Quantification of mean fluorescence intensity (MFI) of DHE staining from three independent experiments. ROS levels were significantly elevated in si-AMPD1-transfected HCT116 cells compared with si-con controls (P = 0.0022). Data are presented as mean ± SD. Student's t-test.

(J) Quantification of intracellular AMP and ATP levels in HCT116 cells transfected with si-con or si-AMPD1. AMPD1 knockdown led to significant accumulation of AMP and a marked reduction in ATP levels (P < 0.0001 for AMP; P < 0.01 for ATP). Data are presented as mean ± SD. Student's t-test.

How to cite this article: Aijie T, Min Z, Yifan Long, Shuai C, Yongguo C. Construction and Validation of a Prognostic Model for Colon Adenocarcinoma Based on Mitochondrial Metabolism-Related Genes. Canc Therapy & Oncol Int J. 2026; 32(1): 556329. DOI: 10.19080/CTOIJ.2026.31.556329

Among the eight core genes selected through LASSO regression, FABP6 and PLAAT2 were significantly downregulated in high-risk groups, while ADH1C, AMPD1, HPGDS, and others showed opposite trends. Previous studies have demonstrated that ADH1C inhibits Wnt/β-catenin signaling through retinol metabolism catalysis; its high expression may represent a compensatory elevation due to functional inactivation (such as mutation or epigenetic silencing), resulting in failure to inhibit the Wnt/β-catenin pathway and ultimately loss of restriction on tumor stem cell self-renewal [34].

AMPD1, as a rate-limiting enzyme in purine metabolism, promotes ATP regeneration through high expression, supporting highly invasive phenotypes [35]. PLAAT2, as a protective gene, may enhance lysophosphatidic acid generation through phospholipase A2 activity, thereby activating the PI3K-Akt-mTOR axis [36]. These mechanisms collectively constitute the molecular foundation of hyperactive tumor metabolism and apoptosis resistance in high-risk groups. Multivariate Cox regression analysis confirmed that risk scores serve as a prognostic factor independent of traditional parameters such as age and TNM stage.

The model achieved AUC values of 0.691–0.749 for predicting 1-year, 3-year, and 5-year survival rates, significantly outperforming previous prediction systems based on single-gene biomarkers. Particularly noteworthy is that the nomogram constructed after incorporating race variables demonstrated precise survival probability prediction capability, providing a practical tool for clinical individualized prognostic assessment. This aligns with recent studies emphasizing the unique value of mitochondrial metabolic genes as "metabolic checkpoints" in tumor prognostic stratification [37,38].

The presence of 14,450 DEGs between high-risk and low-risk groups, combined with GSEA analysis results, collectively reveals the malignant biological nature of high-risk COAD. Regarding metabolic reprogramming, AMPK/mTOR pathway enrichment suggests energy sensing dysregulation, while enhanced oxidative phosphorylation reflects excessive ATP demand in tumor cells [39]. Regarding tumor microenvironment remodeling, Hippo pathway activation may drive matrix fibrosis through YAP/TAZ signaling, while upregulation of "fat digestion and absorption" pathways is associated with lipid provisioning by cancer-associated fibroblasts [40,41].

These findings are consistent with scRNA-seq studies revealing COAD microenvironment characteristics, where enrichment of tissue stem cells and activation of CXCL/TNF signaling networks in high-risk groups may form a tolerant microenvironment through recruitment of immunosuppressive cells (such as Tregs and M2 macrophages) [42], thereby explaining the poor clinical outcomes observed in this patient cohort.

Despite the value of this study in revealing the prognostic utility of mitochondrial metabolism-related genes in COAD through multi-omics integration, several limitations remain:

(1) Mechanistic level: CRISPR knockout or organoid models are required to validate the causal effects of key genes (such as PLAAT2) on mitochondrial-related metabolic flux;

(2) Clinical translation: Prospective cohort validation is needed to verify the model's utility in guiding adjuvant chemotherapy or targeted therapy decisions;

(3) Dynamic monitoring: Future studies could combine plasma mitochondrial DNA mutation profiling to explore the feasibility of real-time tumor burden assessment;

(4) External validation: The prognostic model was developed and tested only within the TCGA cohort. Although the model performed well internally, its generalizability to other populations remains to be confirmed. Independent external validation using datasets such as GEO or ICGC is warranted in future studies.

This study represents the first transformation of mitochondrial metabolism-related gene signatures into a precision prognostic tool for COAD. Its prediction capability independent of traditional staging and its interaction with the tumor microenvironment provide novel perspectives for understanding metabolic-immune co-regulatory networks. This model can serve not only as a supplement to existing TNM staging but also as a theoretical foundation for guiding individualized therapeutic strategies, particularly providing evidence for metabolic-targeted combination regimens in immunotherapy-resistant patients.

Author Contribution

Aijie Tang: Conceptualization, Methodology, Software, Formal analysis, Writing – original draft.

Min Zhao: Data curation, Validation, Investigation.

Yifan Long: Visualization, Software, Resources.

Shuai Cao: Formal analysis, Investigation, Writing – review & editing.

Yongguo Cai: Conceptualization, Supervision, Funding acquisition, Writing – review & editing, Project administration.

Funding

This study was funded by the Zhejiang Provincial Medical and Health Science and Technology Project (Grant No. 2024KY1655).

Conflicts of Interest

The authors declare no conflicts of interest.

Data Availability Statement

The datasets analyzed in this study are publicly available. Transcriptomic and clinical data for colon adenocarcinoma (COAD) were obtained from The Cancer Genome Atlas (TCGA) database (https://gdc.cancer.gov/). The list of mitochondrial

How to cite this article: Aijie T, Min Z, Yifan Long, Shuai C, Yongguo C. Construction and Validation of a Prognostic Model for Colon Adenocarcinoma Based on Mitochondrial Metabolism-Related Genes. Canc Therapy & Oncol Int J. 2026; 32(1): 556329. DOI: 10.19080/CTOIJ.2026.31.556329

metabolism-related genes was downloaded from the MSigDB database (https://www.gsea-msigdb.org/gsea/msigdb). All data used in this study are accessible upon request from the corresponding author.

References

1. Firas Baidoun, Kholoud Elshiwy, Yasmine Elkeraie, Zahi Merjaneh, George Khoudari, et al. (2021) Colorectal Cancer Epidemiology: Recent Trends and Impact on Outcomes. Curr Drug Targets 22(9): 998-1009.
2. Yu L, Zhang MM, Hou JG (2022) Molecular and cellular pathways in colorectal cancer: apoptosis, autophagy and inflammation as key players. Scand J Gastroenterol 57(11): 1279-1290.
3. Fabregas JC, Ramnaraign B, George TJ (2022) Clinical Updates for Colon Cancer Care in 2022. Clin Colorectal Cancer 21(3): 198-203.
4. Alessandro Audisio, Roberta Fazio, Valentina Daprà, Irene Assaf, Alain Hendlisz, et al. (2024) Neoadjuvant chemotherapy for early-stage colon cancer. Cancer Treat Rev 123: 102676.
5. Khan FA, Albalawi R, Pottoo FH (2022) Trends in targeted delivery of nanomaterials in colon cancer diagnosis and treatment. Med Res Rev 42(1): 227-258.
6. Kezhen Yi, Jianyuan Wu, Xuan Tang, Qian Zhang, Bicheng WangX, et al. (2022) Identification of a novel glycolysis-related gene signature for predicting the survival of patients with colon adenocarcinoma. Scand J Gastroenterol 57(2): 214-221.
7. Zhao W, Jin L, Chen P, et al. (2022) Colorectal cancer immunotherapy-Recent progress and future directions. Cancer Lett 545: 215816.
8. Winter JM, Yadav T, Rutter J (2022) Stressed to death: Mitochondrial stress responses connect respiration and apoptosis in cancer. Mol Cell 82(18): 3321-3332.
9. Carmine Rocca, Teresa Soda, Ernestina Marianna De Francesco, Marco Fiorillo, Francesco Moccia, et al. (2023) Mitochondrial dysfunction at the crossroad of cardiovascular diseases and cancer. J Transl Med 21(1): 635.
10. Jacopo Di Gregorio, Sabrina Petricca, Roberto Iorio, Elena Toniato, Vincenzo Flati (2022) Mitochondrial and metabolic alterations in cancer cells. Eur J Cell Biol 101(3): 151225.
11. Kirsten L Bryant, Clint A Stalnecker, Daniel Zeitouni, Jennifer E Klomp, Sen Peng, et al. (2019) Combination of ERK and autophagy inhibition as a treatment approach for pancreatic cancer. Nat Med 25(4): 628-640.
12. Yanni Li, Kristina Sundquist, Naiqi Zhang, Xiao Wang, Jan Sundquist, et al. (2023) Mitochondrial related genome-wide Mendelian randomization identifies putatively causal genes for multiple cancer types. EBioMedicine 88: 104432.
13. Ehsan S, Covarrubias-Zambrano O, Bossmann SH (2022) Mitochondrial Targeting Peptide-based Nanodelivery for Cancer Treatment. Curr Protein Pept Sci 23(10): 657-671.
14. Zhiping Feng, Marisa E Hom, Thomas E Bearrood, Zachary C Rosenthal, Daniel Fernández, et al. (2022) Targeting colorectal cancer with small-molecule inhibitors of ALDH1B1. Nat Chem Biol 18(10): 1065-1075.
15. Zhenyu Zhu, Qingsheng Hou, Bishi Wang, Changhao Li, Luguang Liu, et al. (2022) A novel mitochondria-related gene signature for controlling colon cancer cell mitochondrial respiration and proliferation. Hum Cell 35(4): 1126-1139.
16. Yizhou Wang, Feihong Song, Xiaofeng Zhang, Cheng Yang (2022) Mitochondrial-Related Transcriptome Feature Correlates with Prognosis, Vascular Invasion, Tumor Microenvironment, and Treatment Response in Hepatocellular Carcinoma. Oxid Med Cell Longev 2022: 1592905.
17. Mazandu GK, Chimusa ER, Mulder NJ (2017) Gene Ontology semantic similarity tools: survey on features and challenges for biological knowledge discovery. Brief Bioinform 18(5): 886-901.
18. Yuanbin Jiang, Xin Gou, Zongjie Wei, Jianyu Tan, Haitao Yu, et al. (2020) Bioinformatics profiling integrating a three immune-related long non-coding RNA signature as a prognostic model for clear cell renal cell carcinoma. Cancer Cell Int 20: 166.
19. Yi-Bin Xi, Fan Guo, Zi-Liang Xu, Chen Li, Wei Wei, et al. (2018) Radiomics signature: A potential biomarker for the prediction of MGMT promoter methylation in glioblastoma. J Magn Reson Imaging 47(5): 1380-1387.
20. Li Yu, Li Xiang, Jihua Feng, Bocheng Li, Zhibin Zhou, Ji Li, et al. (2018) miRNA-21 and miRNA-223 expression signature as a predictor for lymph node metastasis, distant metastasis and survival in kidney renal clear cell carcinoma. J Cancer 9(20): 3651-3659.
21. Qingzuo Liu, Ruigang Diao, Guoyan Feng, Xiaodong Mu, Aiqun Li (2017) Risk score based on three mRNA expression predicts the survival of bladder cancer. Oncotarget 8(37): 61583-61591.
22. Ying Qi, Di Chen, Qiqi Lu, Yu Yao, Chunxia Ji (2019) Bioinformatic Profiling Identifies a Fatty Acid Metabolism-Related Gene Risk Signature for Malignancy, Prognosis, and Immune Phenotype of Glioma. Dis Markers 2019: 3917040.
23. Lotte Rasmussen, Nicole Pratt, Morten Rix Hansen, Jesper Hallas, Anton Pottegård (2018) Using the "proportion of patients covered" and the Kaplan-Meier survival analysis to describe treatment persistence. Pharmacoepidemiol Drug Saf 27(8): 867-871.
24. Li Wang, Na Zhou, Jialin Qu, Man Jiang, Xiaochun Zhang (2020) Identification of an RNA binding protein-related gene signature in hepatocellular carcinoma patients. Mol Med 26(1): 125.
25. Vinod P Balachandran 1, Mithat Gonen, J Joshua Smith, Ronald P DeMatteo (2015) Nomograms in oncology: more than meets the eye. Lancet Oncol 16(4): e173-e180.
26. Huang R, Liao X, Li Q (2017) Identification and validation of potential prognostic gene biomarkers for predicting survival in patients with acute myeloid leukemia. Onco Targets Ther 10: 5243-5254.
27. Wanli Yang, Liaoran Niu, Xinhui Zhao, Lili Duan, Yiding Li, et al. (2020) Development and validation of a survival model based on autophagy-associated genes for predicting prognosis of hepatocellular carcinoma. Am J Transl Res 12(10): 6705-6722.
28. In J, Lee DK (2019) Survival analysis: part II - applied clinical data analysis. Korean J Anesthesiol 72(5): 441-457.
29. Hanzelmann S, Castelo R, Guinney J (2013) GSVA: gene set variation analysis for microarray and RNA-seq data. BMC Bioinformatics 14: 7.
30. YunYan Tai, Fengjun Cao, Mingxing Li, Pindong Li, Tao Xu, et al. (2019) Enhanced mitochondrial pyruvate transport elicits a robust ROS production to sensitize the antitumor efficacy of interferon-gamma in colon cancer. Redox Biol 20: 451-457.
31. Mariella Arcos, Lavanya Goodla, Hyeoncheol Kim, Sharina P Desai, Rui Liu, et al. (2025) PINK1-deficiency facilitates mitochondrial iron accumulation and colon tumorigenesis. Autophagy 21(4): 737-753.
32. Kun Liu 1, Shengli Zhou, Ji-Young Kim, Kristin Tillison, David Majors, et al. (2009) Functional analysis of FSP27 protein regions for lipid droplet localization, caspase-dependent apoptosis, and dimerization with CIDEA. Am J Physiol Endocrinol Metab 297(6): E1395-E1413.

How to cite this article: Aijie T, Min Z, Yifan Long, Shuai C, Yongguo C. Construction and Validation of a Prognostic Model for Colon Adenocarcinoma Based on Mitochondrial Metabolism-Related Genes. Canc Therapy & Oncol Int J. 2026; 32(1): 556329. DOI: 10.19080/CTOIJ.2026.31.556329

33. Juan Zhou, Elliot D Mock, Karol Al Ayed, Xinyu Di, Vasudev Kantae, et al. (2020) Structure-Activity Relationship Studies of alpha-Ketoamides as Inhibitors of the Phospholipase A and Acyltransferase Enzyme Family. J Med Chem 63(17): 9340-9359.

34. Qinjunjie Chen, Fengwei Li, Yuzhen Gao, Gaoran Xu, Leilei Liang, et al. (2020) Identification of Energy Metabolism Genes for the Prediction of Survival in Hepatocellular Carcinoma. Front Oncol 10: 1210.

35. Long Wang, Xue Zhang, Mengxue Wang, Yunhai Li, Jiali Xu, et al. (2021) AMPD1 Is Associated with the Immune Response and Serves as a Prognostic Marker in HER2-Positive Breast Cancer. Front Oncol 11: 749135.

36. Boris Rodenak-Kladniew, Agustina Castro, Peter Stärkel, Christine De Saeger, Margarita García de Bravo, et al. (2018) Linalool induces cell cycle arrest and apoptosis in HepG2 cells through oxidative stress generation and modulation of Ras/MAPK and Akt/mTOR pathways. Life Sci 199: 48-59.

37. Bowen Xie, Shuangyan Wang, Nian Jiang, Jian Jian Li (2019) Cyclin B1/CDK1-regulated mitochondrial bioenergetics in cell cycle progression and tumor resistance. Cancer Lett 443: 56-66.

38. Sylvain Delaunay, Gloria Pascual, Bohai Feng, Kevin Klann, Mikaela Behm, et al. (2022) Mitochondrial RNA modifications shape metabolic plasticity in metastasis. Nature 607(7919): 593-603.

39. Wei Liu, Yuechao Zhao, Guangfu Wang, Shuang Feng, Xuhui Ge, et al. (2022) TRIM22 inhibits osteosarcoma progression through destabilizing NRF2 and thus activation of ROS/AMPK/mTOR/autophagy signaling. Redox Biol 53: 102344.

40. Ricardo Gargini, Maribel Escoll, Esther García, Ramón García-Escudero, Francisco Wandosell, et al. (2016) WIP Drives Tumor Progression through YAP/TAZ-Dependent Autonomous Cell Growth. Cell Rep 17(8): 1962-1977.

41. S Kamali Zonouzi, PS Pezeshki, S Razi, N Rezaei (2022) Cancer-associated fibroblasts in colorectal cancer. Clin Transl Oncol 24(5): 757-769.

42. Qingqing Xiao, Xiaotong Li, Yi Li, Zhenfeng Wu, Chenjie Xu, et al. (2021) Biological drug and drug delivery-mediated immunotherapy. Acta Pharm Sin B 11(4): 941-960.

DOI: 10.19080/CTOIJ.2026.31.556329

How to cite this article: Aijie T, Min Z, Yifan Long, Shuai C, Yongguo C. Construction and Validation of a Prognostic Model for Colon Adenocarcinoma Based on Mitochondrial Metabolism-Related Genes. Canc Therapy & Oncol Int J. 2026; 32(1): 556329. DOI: 10.19080/CTOIJ.2026.31.556329